Korean Journal of Remote Sensing, Vol.33, No.4, 2017, pp.411~422
http://dx.doi.org/10.7780/kjrs.2017.33.4.7

ISSN 1225-6161 (Print)
ISSN 2287-9307 (Online)

Article

Spectral Reflectance of Mongsanpo Tidal Flat, Korea, by using Spectroradiometer Experiments and Landsat Data

Bum-Jun Kim*, Sungsoon Lee and Hoonyol Lee***†**

*Korea Ocean Satellite Center, Korea Institute of Ocean Science and Technology
**Geological Research Center, Korea Institute of Geoscience and Mineral Resources
***Division of Geology and Geophysics, Kangwon National University

Abstract : This research aims to analyze spectral reflectance of intertidal zone and its changes under various environmental conditions. We sampled sand of Mongsanpo tidal flat, Korea, and measured its spectral reflectance by using a spectroradiometer under various water contents, compositions and granularity. We also simulated the reflectance of Landsat 7 ETM+ and compared it with an actual satellite data. Five locations were selected for sampling from the coastline towards the ocean. Grain size diminished stepwise from the coastline to ocean direction, while spectral reflectance differed with wavelength. Water contents lowered the overall reflectance especially at the water absorption bands. Spectral reflectance data were then converted into the simulated one by using Landsat 7 ETM+ spectral reflectance function to be compared with the actual Landsat 7 ETM+ images. It showed the decrease of the spectral reflectance due to the increase of moisture contents from seashore towards the ocean. It is shown that Landsat 7 ETM+ imagery can be efficient to extract moisture contents in the tidal flat while compositional analysis needs satellite sensors with much higher spectral resolution.

Key Words : spectral reflectance, Mongsanpo, tidal flat, water content, Landsat

1. Introduction

Various materials have their unique spectral reflectance characteristics. Spectroradiometers have been widely used to analyze spectral reflectance of rocks, water, vegetations, etc. by using sunlight or artificial light sources. Spectral reflectance measurement by using sunlight as a light source has limitations on some spectral bands observed by atmospheric gases while indoor measurements with artificial light source can reduce such noises and errors. Spectral libraries has been collected for over 50 years and are still in active investigation (Cambule *et al*., 2012; Baldridge *et al*., 2008; Hunt and Salisbury, 1970).

The absorption characteristics of a specific wavelength band are different depending on the composition and content ratio of the material. The spectroradiometer can measure the spectral reflectance

Received June 27, 2017; Revised August 14, 2017; Accepted August 21, 2017.
† Corresponding Author: Hoonyol Lee (hoonyol@kangwon.ac.kr)

without external damage to the measurement object by utilizing the light absorption characteristics. Many studies using spectroscopy have been actively conducted. Madani (2011) and Vasques *et al*. (2014) analyzed the distribution of chemical components in the Middle Mesozoic volcanic basin south east of Egypt and analyzed the soil types using physical and biological spectral characteristics. Yinxian *et al*. (2013) analyzed seasonal suspended matter and its changes in rivers. Many studies have also proposed numerical methods for analyzing the absorption characteristics of materials using spectroradiometer (Clark, 1999; Kang *et al*., 1990; Clark and Roush, 1984). However, studies related to the change of spectral reflectance value under various environmental conditions such as water contents, grain size or composition of the tidal flat, especially in Korean peninsula, have not been reported.

In Korea, three sides are surrounded by the sea where wide tidal flats are formed in the western and southern coast. Tidal flats composed of quartz, feldspar and mica are important biomass resources for maintaining marine ecosystems and provide habitats for various marine life forms (Kim *et al*., 2008). Since the late 1980s, dams have been built in the estuaries and landfills have resulted in the destruction and contamination of various marine habitats (Hong, 2003). As modern tidal flats are changing rapidly especially by the artificial factors, it is necessary to characterize and monitor the environment of tidal flats.

Satellite remote sensing has the advantage of being able to analyze the physical properties of a material without direct access to distant objects (Han, 2013). Recently, multi-spectral and hyper-spectral sensors have been developed and technological advances have made it possible to measure the spectral reflectance in a wide wavelength band (Hyun and Park, 2009)

In this study, we sampled sand at Mongsanpo tidal flat, Korea, and analyzed the absorption characteristics of the unique wavelength using the spectroradiometer by giving an artificial environmental change to the material of the intertidal zone. The analysis of particle size, moisture contents, composition ratio and spectral reflectance characteristics were performed for each sampled materials. Spectral response function (SRF) of Landsat 7 ETM + was applied to the measured spectral reflectance to simulate and compare it with the actual satellite data.

2. Study Area and Data

1) Study Area

Mongsanpo tidal flat is located in Taean peninsula, Sogun-ri, Chungcheongnam-do in Korea (Fig. 1). The tidal flat is shaped as a sandy arch and is mainly composed of quartz sand with a width of 500 m and a length of 6 km (Oh, 1998). The tide is semidiurnal with a period of 12 hours and 25 minutes on average. The mean range of tide is about 460 cm. In case of low tide, the slope is gentle enough to see the bottom with maximum width of 3 km. Current velocity increases from the coast to offshore while tidal current changes from reversing current to nearly rotary current (Jang, 2010). The area is well developed with large coastal sand and beach, mostly composed of quartz and feldspar (Kang, 2003).

2) *In Situ* Data

In order to investigate the spectral reflectance characteristics, a total of 5 samples were collected from the coast of Mongsanpo tidal flat, approximately 100 m apart with each other from the coast. The S1, S2, S3, S4, and S5 in Fig. 1 represent the sampling points of each sample, respectively. S1 is an offshore point closest to the land unaffected by seawater and S5 is the farthest from the land. The weather conditions at the time of sampling were windy with slight rain. On July 7, 2013, sampling was started from S5 at 09:50 am (low tide), and ended at S1 at 10:30 am (40 minutes). To

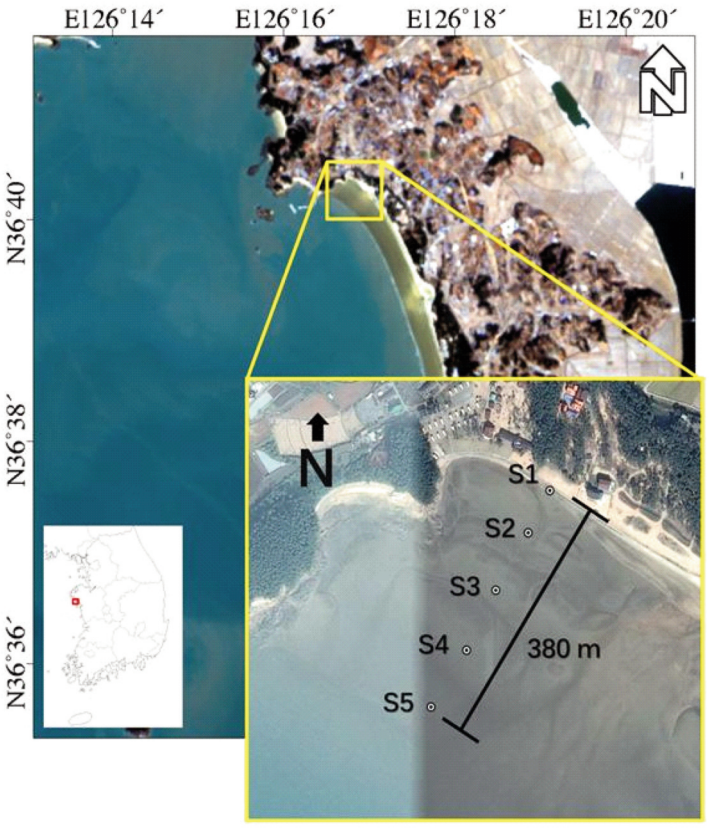

Fig. 1. The study area. The box in the lower left image indicates the location of Mongsanpo tidal flat in Korea (background image: Landsat-8, 2014/01/22). The box in the lower right indicates the five sampling points overlain by Google Earth image.

avoid the deformation and contamination, the samples were immediately sealed into the dark plastic bags.

3) Landsat-7 ETM+ Images

Landsat 7 Enhanced Thematic Mapper Plus (ETM +), which was launched by NASA on April 15, 1999, is an optical satellite currently in operation. Landsat 7 ETM + is a sun-synchronous orbiting satellite capable of imaging at an altitude of 705 km and a width of 185 km, and a revisit interval of 16 days (Mishra *et al*, 2011). The spatial resolution is 30 m and the measurable wavelength range is visible to mid-infrared (0.4 to 2.4 μm) and a thermal band. Landsat 7 ETM+ has eight bands including visible bands (Band 1, 2 and 3), near-infrared bands (Band 4 and 5), thermal bands (Band 6), mid-infrared (Band 7), and a panchromatic band (Band 8). Each band has different wavelength band and different characteristics as shown in Table 1.

Table 1. Summary of Landsat 7 ETM+ sensor parameters (NASA, 2017)

Band	Center Wavelength (μm)	Wavelength Range (μm)	Spatial resolution (m)
1	0.482	0.450 ~ 0.515	30 × 30
2	0.565	0.525 ~ 0.605	30 × 30
3	0.660	0.630 ~ 0.690	30 × 30
4	0.825	0.750 ~ 0.900	30 × 30
5	1.650	1.55 ~ 1.75	30 × 30
6	11.450	10.40 ~ 12.50	60 × 60
7	2.220	2.09 ~ 2.35	30 × 30
8	0.710	0.520 ~ 0.900	15 × 15

3. Methods

1) Sieve Test

In order to observe the change of spectral reflectance due to various environmental changes using spectroradiometer, the particle size of the collected samples was analyzed. This was done using a sieve and a dryer. Five samples of S1, S2, S3, S4, and S5 collected at Mongsanpo tidal flat were completely dried at 200 °C for about 6 hours in a dryer. After drying, 435 g of each sample was extracted, and the particle size was classified using a column of sieves. As there is no particle smaller than 1.18 mm, we have 6 classes in total with the particle size of 1.18 mm to 2.36 mm, 600 μm to 1.18 mm, 300 μm to 600 μm, 150 μm to 300 μm, 75 μm to 150 μm, and less than 75 μm, respectively (Fig. 2).

2) Spectroradiometer Measurement

To analyze the spectral reflectance characteristics according to the environmental changes, spectroradiometer measurement were performed with varying grain size and water contents. The spectroradiometer used in the study is the GER3700 model of the SVC company with the wavelength band from 350 nm to 2500 nm (Slomer, 2005). It has 642 spectral bands with the spectral resolution is 1.5 to 9.5 nm. The spectral resolution decreases toward the mid-infrared (Fig. 3).

Experiments were carried out in a dark room. A

Fig. 2. Sieve test results of Mongsanpo tidal flat.

Wavelength	Spectral resolution
350 nm ~ 1050 nm	1.5 nm
1050 nm ~ 1900 nm	6.5 nm
1900 nm ~ 2500 nm	9.5 nm

Fig. 3. GER3700 spectroradiometer used in this research.

xenon lamp was used as a light source. Xenon lamps have a higher frequency of oscillation than Halogen lamps and therefore have excellent linearity. However, the heat from the lamp is close to 200 °C and there is a risk of deforming the sensors and samples.

To reduce the sample damage and spectral reflectance noise by the xenon lamp, the error was reduced by ventilating the door of the darkroom at every measurement interval. In addition, there are notebooks and batteries to store the measured data from the spectroradiometer. It is essential to maintain the same experimental conditions for each spectral reflectance measurement. Spectral reflectance was measured after fixing the distance between the sensor and the specimen at 8 cm in consideration of the fact that the field of view (FOV) of the spectroradiometer is 10°. The thickness of the samples were made to be 1 cm for all samples (Fig. 4)

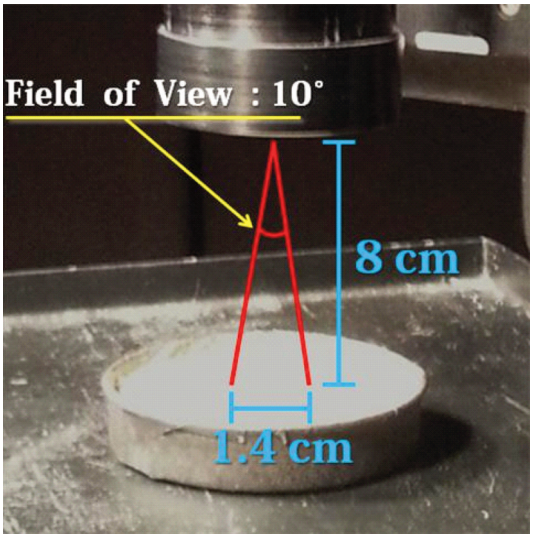

Fig. 4. Measurement setting of the spectroradiometer sensor and the samples.

3) Simulation of Landsat 7 ETM+

In order to analyze the material characteristics in the satellite images, the reflectance values obtained from the images and those measured by the spectroradiometer could be compared. For this purpose, the Spectral Reflectance Function (SRF) of Landsat 7 ETM+ was applied to the spectral reflectance values measured by the spectroradiometer. The GER3700 spectroradiometer system is capable of analyzing the wavelength band from 350 nm to 2500 nm, enabling comparison analysis with SRF of most existing optical satellite sensors. In this study, the spectral reflectance values of the sand flat at Mongsanpo beach were analyzed by applying SRF of Landsat 7 ETM+.

Fig. 5 shows the SRF value of Landsat 7 ETM+ bands. The SRF analysis can be performed by multiplying the spectral reflectance values measured by the spectroradiometer with the SRF values of the corresponding satellites, and then obtaining the average of the respective bands.

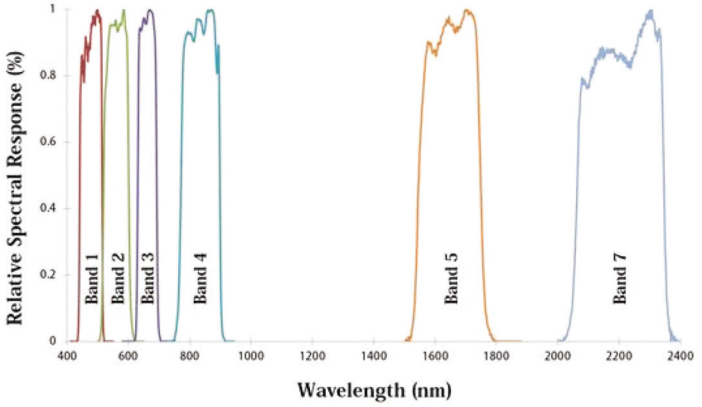

Fig. 5. The spectral response functions (SRFs) of Landsat 7 ETM+ bands.

4. Results and Discussions

1) Classification of Granularity

Grain size of the five locations (S1, S2, S3, S4, S5) in the Mongsanpo tidal flat were analyzed by using sieves and classified into 6 classes such as 1.18 mm to 2.36 mm, 600 μm to 1.18 mm, 300 μm to 600 μm, 150 μm to 300 μm, 75 μm to 150 μm, and <75μm. In places where sea water flows fast, the weight of the soil particles is deposited from heavy ones, and the light weight of the soil particles floats in seawater for a long time and is deposited in a place where the sea water flows slowly (Je *et al*., 2012).

The results of the sieve analysis are shown in Table 2. According to the classification table of sediment particle size, when the particle size of 0.0625 mm ~ 2 mm is more than 90%, it is classified as sandy mud flat (Wentworth, 1919). From the sieve analysis results of Mongsanpo beach, it can be classified as sandy mud flat because the particle size distribution of 0.075 mm ~ 0.3 mm is more than 99%. The ratio of the fine to medium sand (150 μm to 300 μm) decreased from 45.21% at S1 to 4.28% at S5 while those of very fine to fine sand increased from 53.68% at S1 to 94.99% at S5. Therefore, grain size diminished from the high tide area (S1) to the low-tide (S5) area. This result is consistent with the observation of the nearby Chunsu Bay, West coast of Korea, where beach sediments are originated from the sea-cliff erosion and transported by longshore current (Ryu *et al*., 2005).

2) Spectral Reflectance of Samples

Fig. 6 shows the spectral reflectance curves of S1, S2, S3, S4, and S5 samples measured by a spectroradiometer. Spectral reflectance value from visible to short infrared region (400 nm - 1600 nm) decreases from S1 to S5. This is because fine grain particles are increasingly abundant from S1 to S5 and the spectral reflectance decreases due to increased adsorption of light by dark minerals.

No specific correlation was found for the spectral reflectance values longer than 1600 nm. This is thought to be caused by the difference in the fine components of the sediments. The silicate minerals or their compounds such as biotite and hornblende, which are mafic minerals, have low spectral reflectance values in the broad wavelength around 1000 nm. Meanwhile carbonate minerals such as calcite, muscovite have lower spectral reflectance value in the long wavelength band (2300 nm ~ 2500 nm) (Kang *et al*., 1990). The smaller the particles constituting the soil, the more attractive the fine particles of potassium and calcium ions. These ions adhere to the soil particles and do not fall off easily, so they maintain the fertility of the soil by supplying abundant nutrients (Marsh and Dozier, 1981). It is necessary to perform qualitative and quantitative analysis on the sample through X-ray fluorescence spectroscopy (XRF) analysis and modal compositions analysis.

The effect of water contents have played an important role in the decrease of spectral reflectance from S1 to S5. The effect of moisture contents to

Table 2. Sieve test result of the five sampling points of Mongsanpo tidal flat (* nomenclature after USDA soil particle size scale)

Name*	Grain size	S1	S2	S3	S4	S5
very coarse sand/gravel	1.18 mm ~ 2.36 mm	0.10%	0.47%	0.02%	0.08%	0.01%
coarse to very coarse sand	600 μm ~ 1.18 mm	0.13%	0.44%	0.05%	0.10%	0.03%
medium to coarse sand	300 μm ~ 600 μm	0.72%	0.82%	0.34%	0.32%	0.06%
fine to medium sand	150 μm ~ 300 μm	45.21%	46.52%	27.36%	18.45%	4.28%
very fine to fine sand	75 μm ~ 150 μm	53.68%	51.57%	71.64%	80.71%	94.99%
very fine sand	< 75 μm	0.16%	0.18%	0.59%	0.34%	0.66%

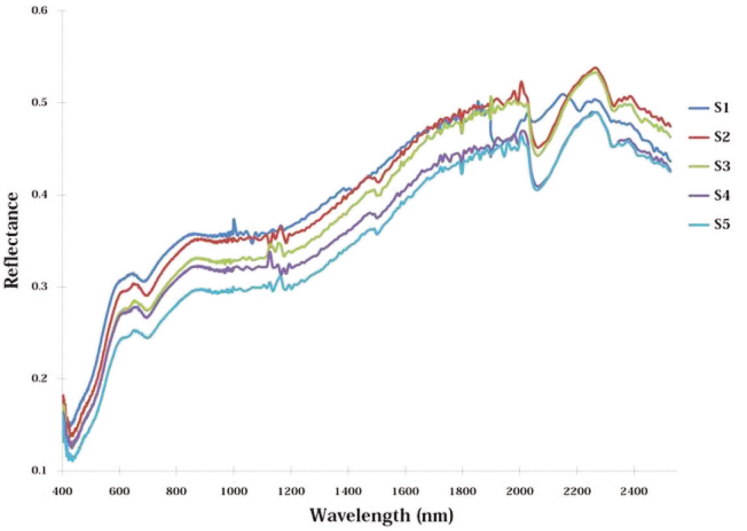

Fig. 6. Reflectance spectra of samples from Mongsanpo tidal flat measured by a spectroradiometer.

spectral reflectance curve is analyzed in the following section.

3) Spectral Reflectance with Varying Moisture Contents

In order to analyze the response characteristics of sand in Mongsanpo tidal flat to moisture contents, spectral reflectance analysis was performed using the sample at S2 with various moisture content set to 0%, 3%, 11%, 17% and fully saturated one (Fig. 7). Spectral reflectance value at a moisture content of 3% were observed to be reduced by half when compared with no water (dry). The particle size of the sample S2 used in the analysis of the water content of the sand tidal flats was 46.52% from 75 μm to 150 μm and 51.57% from 150 μm to 300 μm. Generally, the finer the soil particle size, the higher the water holding capacity, resulting in dramatic decrease of spectral reflectance especially in the water absorption bands with a slight increase of water contents (Chae *et al*., 2000). Therefore, slight

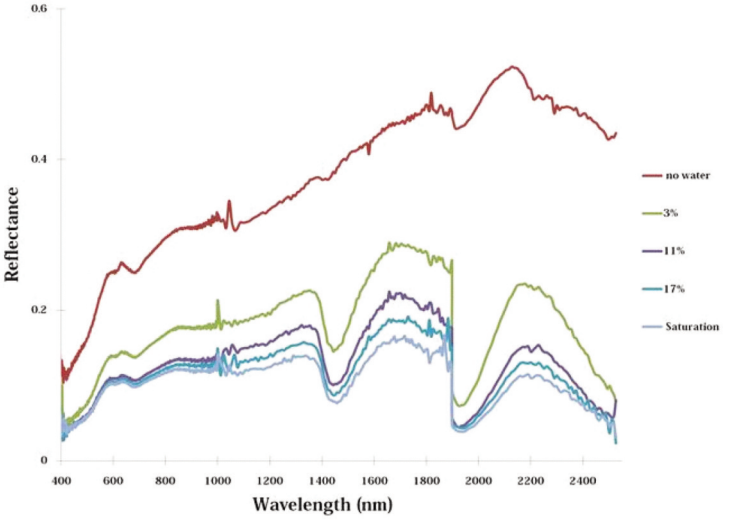

Fig. 7. Reflectance spectra with varying water contents of Mongsanpo tidal flat (sample number: S2).

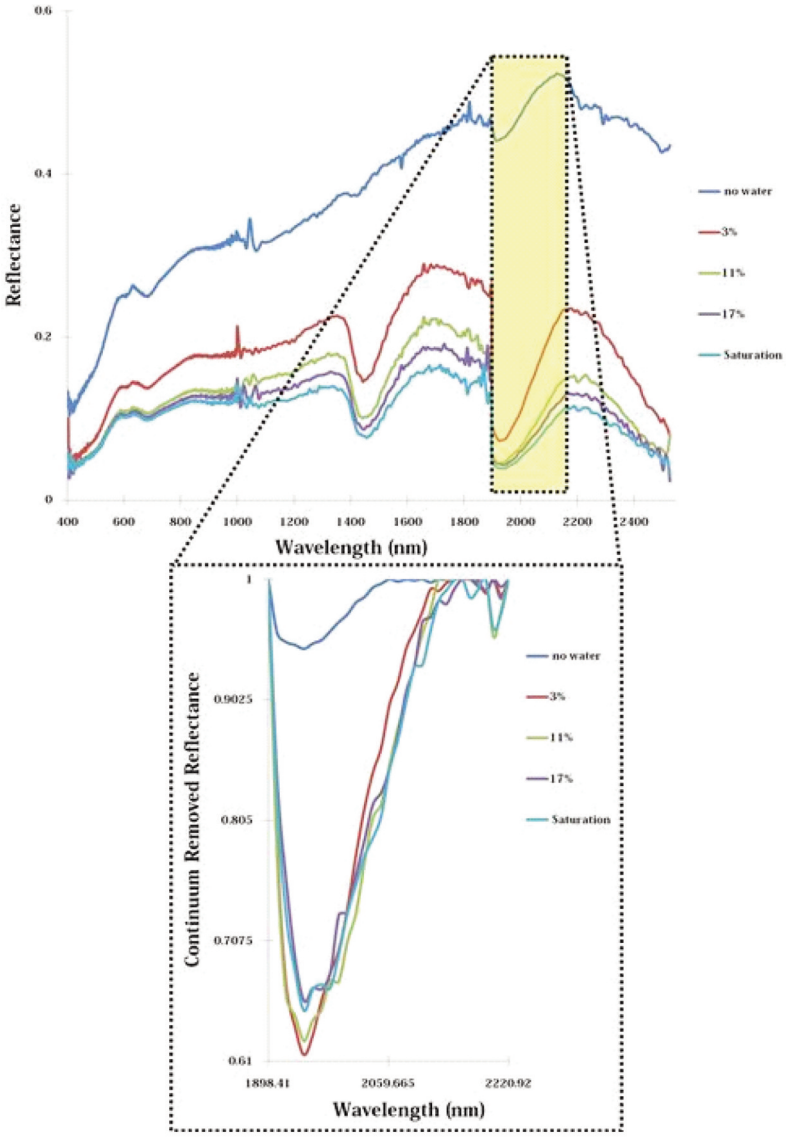

Fig. 8. Continuum-removed reflectance spectra of different water contents of Mongsanpo tidal flat (sample numer: S2).

decrease of spectral reflectance from S1 to S5 in Fig. 6 is thought to be originated from fine mineral composition rather than moisture contents.

The band depth and band area were calculated after the continuum removal of the wavelength band from 1898 nm to 2220 nm, where the absorption characteristics of water and hydroxide ions appears (Fig. 8). The difference in spectral reflectance between the no water condition and when water is added can be clearly distinguished. Relative band depth and band area values clearly distinguish the spectral reflectance differences of moisture content of 3%, 11%, 17% and saturation (Fig. 9). At 3% moisture addition, the band depth and band area show a sharp increase. After that, the band area shows a slight increase and then decrease while the band depth shows a slight decrease continuously.

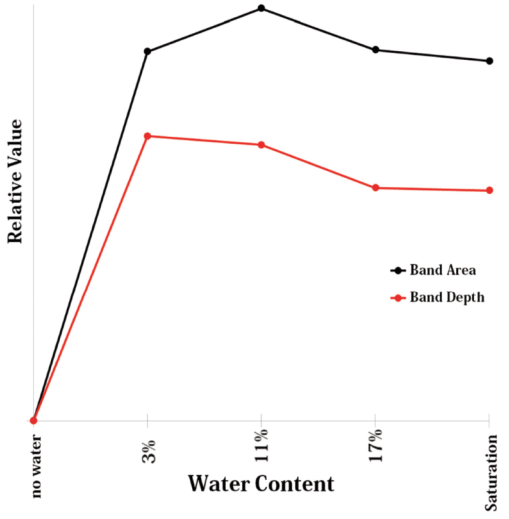

Fig. 9. Band area and band depth of the spectral reflectivity with varying water contents of Mongsanpo tidal flat.

4) Simulation of Spectral Reflectance of Landsat 7 ETM+

We simulated the Landsat 7 ETM+ spectral reflectance from the S2 points of Mongsanpo tidal flat with varying water content (Fig. 10) As the water content increases, the overall spectral reflectance decreases. Especially, the decrease in the band 5 and band 7 of the mid-infrared wavelength is significant. It was impossible to analyze detailed spectral characteristics near 1400 nm and 1900 nm which are the water absorption bands due to the small number of bands and low spectral resolution. However, spectral characteristics in band 5 and band 7 is relatively larger, so it is expected that we can identify the influence of water contents in this bands.

5) Comparison with Landsat 7 ETM+ image

Landsat 7 ETM+ satellite images were then used to analyze the spectral reflectance characteristics of the Mongsanpo tidal flat. No Landsat 7 ETM+ image could be obtained at the same time as in situ dataset, and images with similar dates could not be analyzed because of heavy cloud. Therefore, considering the water condition of Mongsanpo tidal flat at the time of collecting samples, we used images obtained on April 20, 2014 (Fig. 11).

W1 ~ W6 in Fig. 11 show the sampling point of the sands in the Mongsanpo tidal flat. W1 is a coastal beach

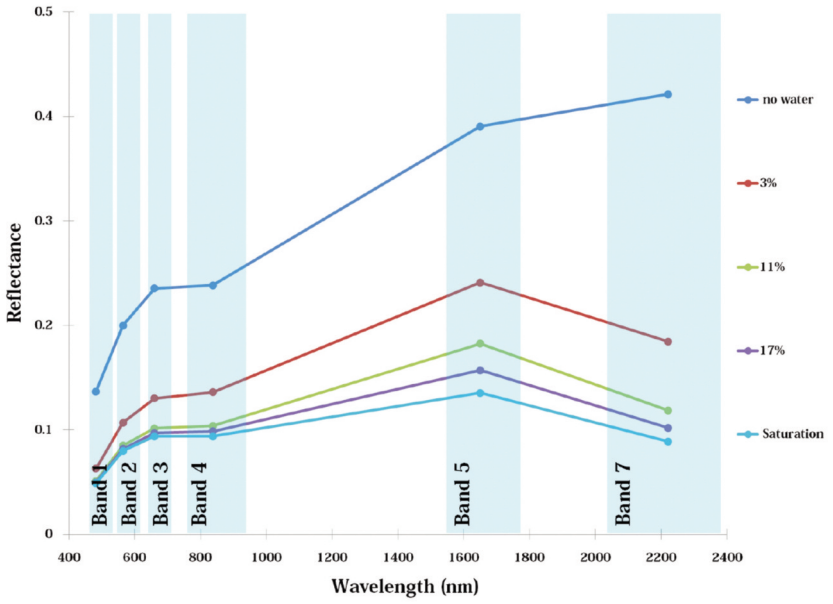

Fig. 10. Spectral response functions of spectroradiometer measurements equivalent to Landsat 7 ETM+ with varying water contents of Mongsanpo tidal flat (sample number: S2).

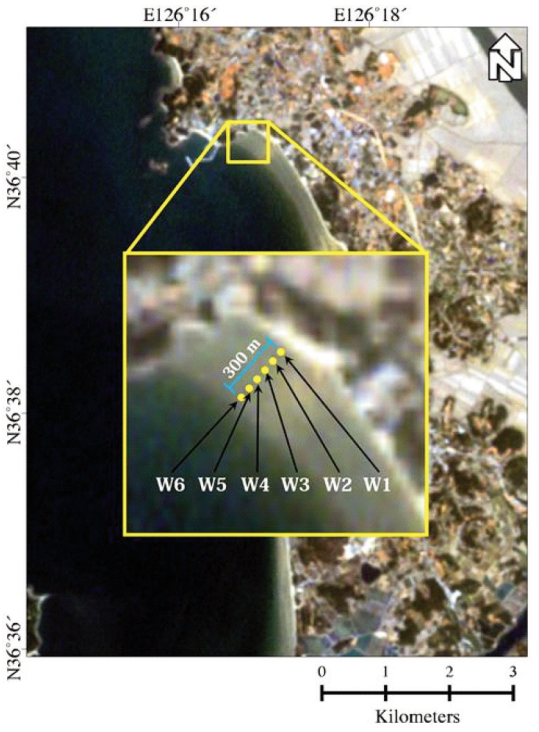

Fig. 11. Sampling locations of Mongsanpo tidal flat in the Landsat-7 ETM+ image acquired on 20 April 2014.

point nearest to the inland while W6 is the most seaward point. In the case of the intertidal zone, W6 in the ocean direction has a larger water content than W1 due to the time difference in the water level dropping from the high tide to the low tide. Fig. 12 shows the spectral reflectance of W1 ~ W6 at Landsat 7 ETM+ satellite image. It can be confirmed that the spectral reflectance of W6 point is lowest due to high water content, showing similar trend with the simulated one in Fig. 10. It is also confirmed that the spectral reflectance decreases in band 5 and band 7 compared to band 1 ~ band 4.

5. Conclusion

In this study, spectral reflectance characteristics of sandy flat in Mongsanpo tidal flat under various environmental factors were investigated by using a spectrophotometer and Landsat 7 ETM+ image. The particle size distribution of fine granules increased from inland (S1) to offshore (S5). The spectral reflectance (400nm - 1600 nm) decreased from S1 to S5 partially due to higher adsorption of silicate minerals (potassium and calcium) in the shorter wavelength region. No specific correlation was found for the spectral reflectance values longer than 1600 nm. As a result of water content measurement, the spectral reflectance of the S2 decreased as the water content increased.

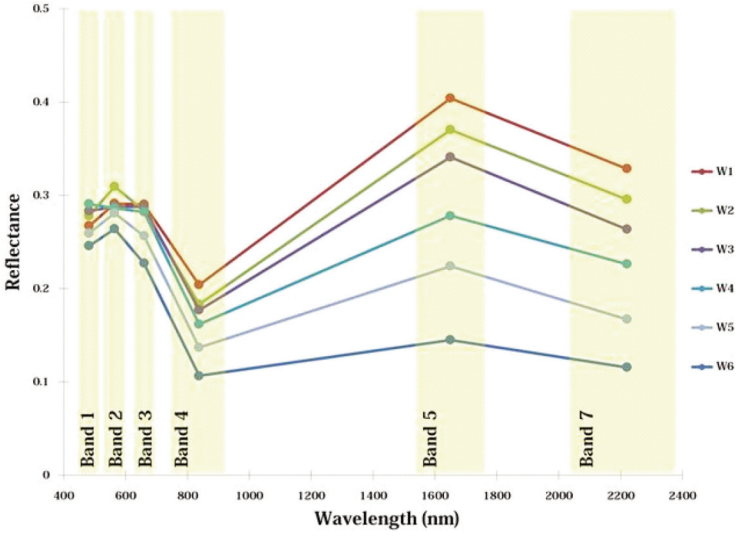

Fig. 12. Spectral reflectance of the Landsat 7 ETM+ sensors of Mongsanpo tidal flat.

Therefore, the spectral reflectance may be slightly reduced due to the increase of the moisture content from S1 to S5.

By applying Landsat 7 ETM+ SRF to each sample, it was possible to clearly distinguish the change and difference in the overall value of spectral reflectance. However, due to the small number of bands, it would be difficult to analyze the absorption characteristics at specific wavelengths. Comparison of the simulated and the actual Landsat 7 ETM+ satellite image showed that moisture content increases toward the sea side. The result showed a possibility of extracting the moisture content of the sand tidal flat through the satellite image.

Landsat 7 ETM+ satellite imagery, however, lacks detailed analysis of the absorption band and components due to the limitations of low spectral resolution. In the future, it is considered possible to analyze the composition of sand tidal flat by applying the SRF of the satellite sensors equipped with hyperspectral sensor.

Acknowledgements

This research was supported by the National Research Foundation of Korea (NRF-2016R1D1A1A09916630) and the 2016 Research Grant from Kangwon National University (No. 520160323).

References

Baldridge, A. M., S. J. Hook, C. I. Grove, and G. Rivera, 2008. The ASTER spectral library version 2.0, *Remote sensing of Environment*, 113(4): 711-715.

Cambule, A. H., D. G. Rossiter, J. J. Stoorvogel, and E. M. A. Smaling, 2012. Building a near-infrared spectral library for soil organic carbon estimation in the Limpopo National Park, *Mozambique, Journal of Geoderma*, 183: 41-48.

Chae H. S., G. E. Kim, S. J. Kim, Y. S. Seop, G. S. Lee, G. S. Jo, and M. H. Jo, 2000. *Environmental Remote Sensing*, Sigmapress, Seoul, Republic of Korea (in Korean with English abstract).

Clark R. N., 1999. *Chapter 1: spectroscopy of rocks and minerals, and principles of spectroscopy, Manual of Remote Sensing, Remote Sensing for the Earth Sciences*, Wiley, New York, USA, pp. 3-58.

Clark R. N. and T. L. Roush, 1984. Reflectance spectroscopy: Quantitative analysis techniques for remote sensing applications, *Journal of Geophysical Research*, 89(B7): 6329-6340.

Han H. S., 2013. *Studies on backscattering of lake ice and tidal deformation and radiation characteristics of glacier using microwave remote sensing*, Doctoral dissertation, University of Kangwon, Republic of Korea (in Korean with English abstract).

Hong J. S., 2005. *The Korean tidal flats*, Daewonsa, Seoul, Republic of Korea (in Korean with English abstract).

Hunt G. R. and J. W. Salisbury, 1970. Visible and near-infrared spectra of minerals and rocks, *Modern Geology*, 1: 283-300.

Hyun C. U. and H. D. Park, 2009. Spectral analysis of mineral materials for mineral exploration, The Korean Society of Remote Sensing conference 2009, Seoul, Republic of Korea, Mar. 27, pp. 318-322 (in Korean with English abstract).

Jang S. Y., 2010. *Observation of ridge-runnel and ripples in Mongsanpo intertidal flat by satellite SAR imagery*, Master dissertation, University of Kangwon, Republic of Korea (in Korean with English abstract).

Je J. G., J. Kim, H. J. Kim, S. M. Park, S. B. Park, J. H. Seo, G. S. Lee, and H. G. Lee, 2012. *Understanding and Education of Tidal Flats*, Korea Marine Pollution Response Corporation,

Seoul, Republic of Korea (in Korean with English abstract).

Kahng T. G., 2003. The origin of coastal dunesand in the Chungcheongnam-do, *The Korean Geographic Society*, 38(4): 505-517 (in Korean with English abstract).

Kang P. C., M. J. Cho, and B. J. Lee, 1990. Spectral analysis of igneous and sedimentary rocks, *Korean Journal of Remote Sensing*, 6(1): 49-62 (in Korean with English abstract).

Kim J. G., S. J. You, and O. I. Choi, 2008. Evaluation of heavy metals pollution and characteristics of particle composition for tidal flat sediments in Julpo Bay, *Journal of the Korean Society of Marine Environment and Satety,* 14(4): 247-256 (in Korean with English abstract).

Madani A. A., 2011. Spectral properties of carbonatized ultramafic mantle xenoliths and their host olivine basalts, Jabal Al Maqtal basin, south eastern desert, Egypt, using ASD fieldSpec spectroradiometer, *The Egyptian Journal of Remote Sensing and Space Sciences*, 14(1): 41-48.

Marsh W. M. and J. Dozier, 1981. *Landscape, an introduction to physical geography*, Addison Wesley, MA, USA, p. 637.

Mishra R.K., P. P. Bahuguna, and V. K. Singh, 2011. Detection of coal mine fire in Jharia Coal Field using Landsat-7 ETM+ data, *International Journal of Coal Geology*, 86(1): 73-78.

NASA, 2017. Landsat 7 Science Data Users Handbook, available online at https://landsat.gsfc.nasa.gov/wp-content/uploads/2016/08/Landsat7_Handbook.pdf.

Oh J. K. and B. C. Kum, 1998. Sedimentologic characteristics of macrotidal beach in Mongsanpo, west coast of Korea, *Korean Earth Science Society*, 19(3): 310-317 (in Korean with English abstract).

Ryu J. H., Y. H. Ahn, H. J. Woo, C, H, Park, H. R. Yoo, and J. S. Won, 2005. Qualitative classification of the surface sedimentary facies of tidal flat using high resolution satellite data: A case study of Hwangdo tidal flat in Cheonsu Bay, *Journal of the Geological Society of Korea*, 41(2): 199-210 (in Korean with English abstract).

Slomer L., 2005. *GER 3700 User Manual, Release 3.2*, Spectra Vista Corporation, Poughkeepsie, NY, USA

Vasques G. M., J. A. M. Dematte, R. A. Viscarra Rossel, L. Rairez-Lopez, and F. S. Terra, 2014. Soil classification using visible/near-infrared diffuse reflectance spectra from multiple depths, *Journal of Geoderma*, 223: 73-78.

Wentworth C. K., 1919. A laboratory and field study of cobble abrasion, *Journal of Geology*, 27(7): 507-521.

Yinxian S., J. Ji, C. Mao, G. A. Ayoko, and R. L. Frost, 2013. The use of reflectance visible-NIR spectroscopy to predict seasonal change of trace metals in suspended solids of Changjiang River, *Catena*, 109: 217-224.